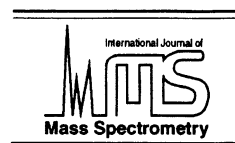




ELSEVIER

International Journal of Mass Spectrometry 198 (2000) 77–82



Absolute electron capture cross sections of Kr^+ with Ne atoms

H. Martínez^{a,*}, P.G. Reyes^b, J.M. Hernández^c, B.E. Fuentes^b

^aCentro de Ciencias Físicas, UNAM, Apartado Postal 48-3, 62191, Cuernavaca, Morelos, México

^bFacultad de Ciencias, UNAM, México D. F., México

^cFacultad de Ciencias, UAEMex., Toluca, Estado de México, México

Received 6 August 1999; accepted 21 December 1999

Abstract

The absolute differential and total cross sections for single electron capture at energies between 1 and 5 keV are reported. The reduced differential cross sections scale reasonably well, showing an overall increase of two orders of magnitude and three maxima at different collision energies. We deduce, from the experimental differential cross section, that the electron capture channel “opens” at a critical projectile-target separation between $2.88 a_0$ and $3.15 a_0$ and that at least two different processes are involved in the present energy range. The single electron capture cross section of Kr^+ ions in various media is shown. It has been found that the dependence of the single electron capture cross section with the nuclear charge of the target atoms is oscillatory. (Int J Mass Spectrom 198 (2000) 77–82) © 2000 Elsevier Science B.V.

Keywords: Electron transfer; Angular distributions; Absolute cross sections; Kr^+ ; Kr^0

1. Introduction

Collision studies provide information on the interactions that occur between a given projectile and target [1–3]. Experimental results can be used to test underlying theories and in many cases guide their development. In this context there is substantial literature on keV energy collisions containing, basically, studies of ion–atom problems. Although keV energy ion–atom collisions have been studied for a number of years, our understanding of them remains limited. Except for a few cases, the interpretation of the experimental results is based on a qualitative approach [2,3]. For low-energy collisions of singly charged krypton ions with atomic and molecular

targets, several studies [4–6] have been performed to investigate the potentials of the quasimolecular system formed in these collisions, and to examine the curve-crossing mechanism that plays such an important role in the inelastic processes. Most experiments concerned with the measurement of single electron capture cross sections for Kr^+ [7] have been performed at energies below 350 eV. There has also been a continuous interest in energy-transfer reactions between rare gas (RG) metastable atoms and RG ions because of their applicability to the pumping of rare gas ion lasers [8–10]. In previous articles [11–14] we have reported cross section measurements on the Kr^+ –He, Kr^+ –Ar, Kr^+ –Kr, and Kr^+ –Xe systems. To complement these studies and to provide more information on single electron capture in Kr^+ + RG reactions, we now report absolute total cross sections of single electron capture for Kr^+ collisions with Ne.

* Corresponding author. E-mail: hm@fis.unam.mx

The energy range of the present study is 1–5 keV. In addition, we present the results of the total electron capture cross section as a function of the target atomic number (Z_t) at several incident energies.

2. Experiment

The experiment was carried out at the low-energy accelerator of Centro de Ciencias Físicas, UNAM. A detailed description of the experimental approach has been given in a previous article [15]. Briefly, the Kr^+ ions formed in an arc discharge source are accelerated from 1–5 keV, and selected by a Wien velocity filter. The Kr^+ ions then pass through a series of collimators before entering the gas target cell. The target cell is located at the center of a rotatable computer controlled vacuum chamber that moves the whole detector assembly, which is located 47 cm away from the target cell. A precision stepping motor ensures a high repeatability in the positioning of the chamber over a large series of measurements. The detector assembly consisted of a Harrower-type parallel-plate analyzer and two channel-electron multipliers (CEMs) attached to its exit ends. The neutral beam (Kr^0) passes straight through the analyzer and impinges on a CEM so that the neutral counting rate can be measured. Separation of charged particles occurs inside the analyzer, which is set to detect the Kr^+ ions with the lateral CEM. The CEMs were calibrated in situ with low-intensity Kr^0 and Kr^+ beams that were measured as a current in a Faraday cup by a sensitive electrometer. The uncertainty in the detector calibration was estimated to be less than 3%. A retractable Faraday cup, located 33 cm away from the target cell, allows the measurement of the current of the incoming Kr^+ ion beam.

During the laboratory angular distribution experiment, the collimator in front of the lateral CEM was an orifice of 1 cm in diameter. Under the thin target conditions used in this experiment, the differential cross sections for the Kr^0 formation were evaluated from the measured quantities by the expression

$$\frac{d\sigma(\theta)}{d\Omega} = \frac{I_f(\theta)}{I_0 n l} \quad (1)$$

where I_0 is the number of Kr^+ ions incident per second on the target; n is the number of RG atoms per unit volume (typically 1.2×10^{13} atoms/cm³); l is the length of the scattering chamber ($l = 2.5$ cm); and $I_f(\theta)$ is the number of Kr^0 atoms per unit solid angle per second detected at a laboratory angle θ with respect to the incident beam direction. The total cross section σ for the production of the Kr^0 particles was obtained by the integration of $d\sigma/d\Omega$ over all angles; this is

$$\sigma = 2\pi \int_0^\pi \frac{d\sigma}{d\Omega} \sin(\theta) d\theta \quad (2)$$

In the present work changes were not observed in the absolute values with respect to the ions' source conditions. Also, no variation in the distributions was detected over a target pressure of 0.2–0.6 mTorr.

Several runs were made at different gas target pressures and $d\sigma/d\Omega$ was determined for each run. These values were compared in order to estimate the reproducibility of the experimental results as well as to determine the limits of the “single-collision regime” because the differential and total cross sections reported are absolute.

Several sources of systematic errors are present and have been discussed in a previous article [15]. The absolute error of the reported cross sections is believed to be less than $\pm 15\%$; this represents both random and systematic errors.

3. Results and discussion

Measurements of differential cross sections (DCS) were performed at laboratory angles of $-2.5^\circ \leq \theta \leq 2.5^\circ$ and collision energies of $1.0 \leq E_{\text{lab}} \leq 5.0$ keV. We show in Fig. 1 the measurements of the differential cross sections for Kr^+ ions in Ne at different collision energies (the vertical error bar is of the order of the size of the symbols used in the figure). All curves plotted in Fig. 1 show a monotonic decrease in the differential cross section with increasing angle. The electron capture data show small scale structures in the differential cross sections. Angular and energy

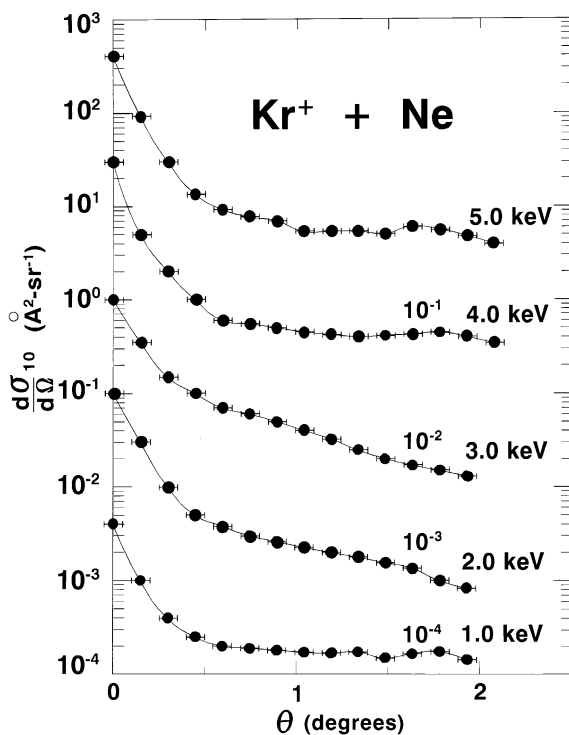


Fig. 1. Measured absolute differential cross sections for single electron capture of Kr^+ on Ne.

dependences of the DCS $\rho = (d\sigma/d\Omega)\theta \sin(\theta)$ of one electron charge transfer in the laboratory system are presented in Fig. 2 where the abscissa is the reduced angle $\tau = E_{\text{lab}}\theta$. The curves representing the reduced differential cross sections (RDCS) for the different energies have an overall increase of two orders of magnitude. At all the energies studied $\rho(\tau)$ has a rather similar behavior within the experimental uncertainty; the general behavior for these curves can be approximated by common curves [16] that are shown as solid lines in Fig. 2. A systematic horizontal shift can be observed between the low-energy curves and the high-energy curves. The results at 2, 3, and 5 keV have a vestige of structure at 3.2, 4.8, and 9.8 keV deg, respectively, whereas such a clear behavior cannot be observed in the RDCs at 1 and 4 keV.

In small-angle scattering processes, the most important observable is the reduced scattering angle τ that is related to the impact parameter b by a functional form—the reduced deflection function—that

depends on the potential. The small-angle reduced cross sections were computed using an exponential shielded Coulomb potential given by [16]

$$V(r) = \frac{Z_p Z_t}{r} \exp\left(-\frac{r}{c}\right) \quad (3)$$

where c was evaluated using the relation $c = a_0[Z_p^{2/3} + Z_t^{2/3}]^{-1/2}$, where a_0 is the Bohr radius, Z_p is the projectile atomic number, and Z_t is the target atomic number; the impact parameter b was evaluated using the reduced functions τ_0 versus (b/c) given in [16]. Because the impact parameter b and the distance of closest approach r_0 are essentially the same in small angle scattering, the features localized at a specific reduced angle τ_x represent interactions at some localized place $\tau_x \approx b_x$ on the potential $V(r)$. In the inelastic scattering, perturbations were observed at certain localized values of τ , which provide us with knowledge of the points of the crossing of the potential curves. Our experimental results show the presence of three maxima apparently centered near 3.2 (at 2 keV), 4.8 (3 keV), and 9.8 (5 keV) keV deg, which provide evidence of three impact parameters at $b \approx 3.15, 3.05,$ and $2.88 a_0$ at an energy $V = 0.034, 0.052,$ and 0.107 eV, respectively. These results suggest that when the Kr^+ projectile penetrates a critical projectile-target separation between 2.88 and $3.15 a_0$, the electron capture channel “opens.”

The measured differential cross sections for single electron capture of Kr^+ impacting on Ne were integrated over the observed angular range; they are listed in Table 1. The behavior of these data will be analyzed later (Fig. 4). We present in Fig. 3 the total single electron cross section of Kr^+ ions in Ne as a function of the incident energy. Error bars are given as an indication of the maximum reproducibility of the data in the present energy range. The curve displays a vestige of an oscillatory behavior with two maxima at 1.5 and 3.5 keV. Because we are reporting the maxima reproducibility of the data, we believe that this behavior is real. Previous investigations also reveal structures at low energies in $\text{Ne}^+ + \text{Ar}$ [7] and $\text{Kr}^+ + \text{Ar}$ reactions [7,13]. Although from the present studies it is not possible to identify the specific

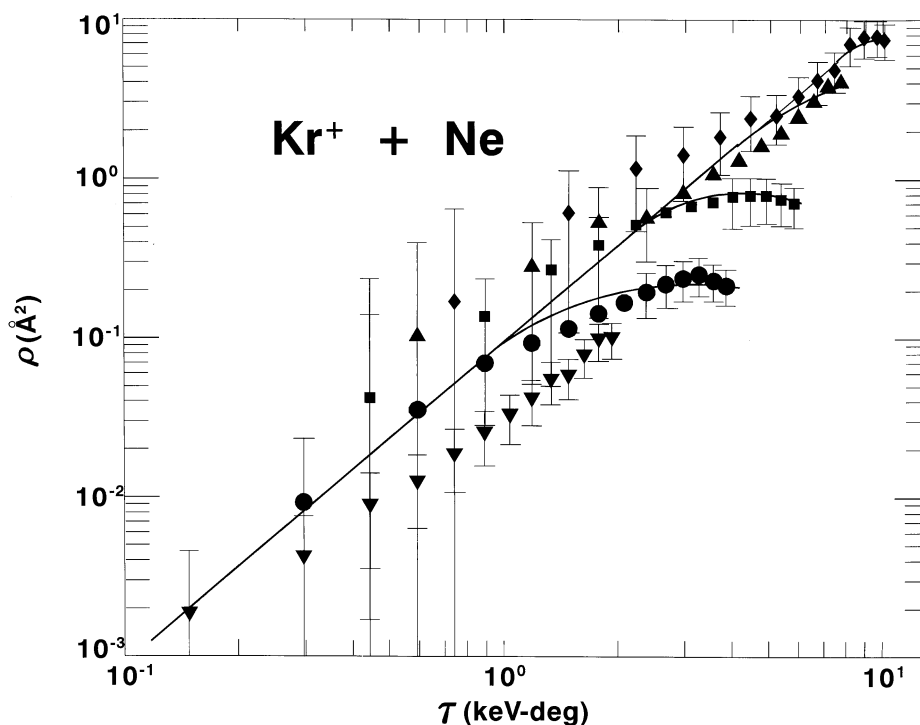


Fig. 2. Reduced differential cross sections for single-electron capture of Kr^+ ions in Ne. Down-pointing triangles, 1.0 keV; circles, 2.0 keV; squares, 3.0 keV; triangles, 4.0 keV; diamonds, 5.0 keV.

processes, the shape of the data in Figs. 2 and 3 suggests that at least two different processes are involved.

There exist several endothermic reactions requiring a minimum collision energy. The Kr^0 atoms are most probably formed in their lowest excited states, characterized by the following transitions: $\text{Kr}^+(4s^2p^5) + \text{Ne}(2s^2p^6) \rightarrow \text{Kr}(4p^6) + \text{Ne}^+(2s^2p^5)$ $\Delta E = -7.563$ eV; $\text{Kr}^+(4s^2p^5) + \text{Ne}(2s^2p^6) \rightarrow$

$\text{Kr}(4p^5(^2P_{11/2}^0)5s) + \text{Ne}^+(1s^22s^2p^5)$ $\Delta E = -17.480$ eV; $\text{Kr}^+(4s^2p^5) + \text{Ne}(2s^2p^6) \rightarrow \text{Kr}(4p^5(^2P_{11/2}^0)5p) + \text{Ne}^+(1s^22s^2p^5)$ $\Delta E = -18.868$ eV; $\text{Kr}^+(4s^2p^5) + \text{Ne}(2s^2p^6) \rightarrow \text{Kr}(4p^5(^2P_{11/2}^0)4d) + \text{Ne}^+(1s^22s^2p^5)$ $\Delta E = -19.563$ eV; ΔE being the energy defect. It is important to mention that because of the ion source used, our beam must contain both $\text{Kr}^+(2P_{1/2})$ and $\text{Kr}^+(^2P_{3/2})$ ions, but we cannot distinguish between these states. The reaction probability decreases with higher endothermicity up to the first ionization limit; hence, these reactions involve a one-electron process in which the Kr^0 atom is in a state with an electronic configuration of $4p^6$, $4p^55s$, $4p^55p$, or $4p^54d$. The type of target cell and the operation conditions (pressure, temperature) leads us to the assumption that Ne^+ is in its ground state.

The total electron capture cross section as a function of the target atomic number (Z_t) for laboratory energies between 1 and 5 keV is shown in Fig. 4. All

Table 1
Electron capture cross section for Kr^+ on Ne

Energy (keV)	$\sigma(\text{\AA}^2)$
1.0	0.007
1.5	0.010
2.0	0.009
2.5	0.015
3.0	0.022
3.5	0.023
4.0	0.022
4.5	0.019
5.0	0.028

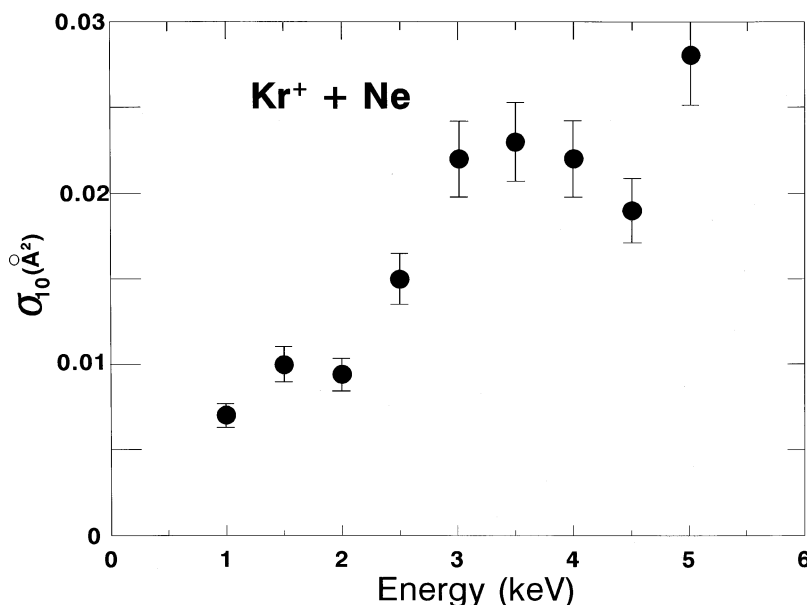


Fig. 3. Total single electron capture cross sections for Kr^+ –Ne collisions.

the curves display the same oscillatory behavior, having a cross section maximum at $Z_t = 36$. Electron capture rapidly decreases and shows a minimum at $Z_t = 10$, following a pronounced structure. An analogous oscillation in the dependence of the cross sections on the nuclear charge Z_t of the target atoms was previously observed by Dimitriev et al. [17] and by Bell and Betz [18]. They calculated the cross section for electron capture to the K shell of Cl ions with an energy of 120 MeV using the Brinkman–Kramers formula and found a nonmonotonic dependence on Z_t . The present experimental results confirm the prediction of the Oppenheimer–Brinkman–Kramers calculation that states that the oscillations in the capture cross sections must also be observed at velocities down to $v \sim v_0$ ($v_0 = 2.18 \times 10^8$ cm/s).

4. Conclusions

We have presented values of absolute differential and total cross sections for single electron capture of Kr^+ in Ne at impact energies between 1 and 5 keV. The results of the present work can be summarized as

follows: (1) The reduced differential cross sections scale reasonably well, showing an overall increase of two orders of magnitude and three maxima at different collision energies. (2) From the experimental differential cross section we deduced that the electron capture channel “opens” at a critical projectile–target separation between $2.88 a_0$ and $3.15 a_0$, where at least two different processes are involved in the present energy range. (3) The total cross section displays an oscillatory behavior and presents two maxima at 1.5 and 3.5 keV. The shape of the data suggests that at least two different processes are involved. (4) We show the single electron capture cross section of Kr^+ ions in various media and the oscillatory dependence of the single electron capture cross section on the nuclear charge of the target atoms.

Acknowledgements

We wish to thank A. González for his technical assistance. Research supported by CONACYT 32175-E and DGAPA-IN-109303.

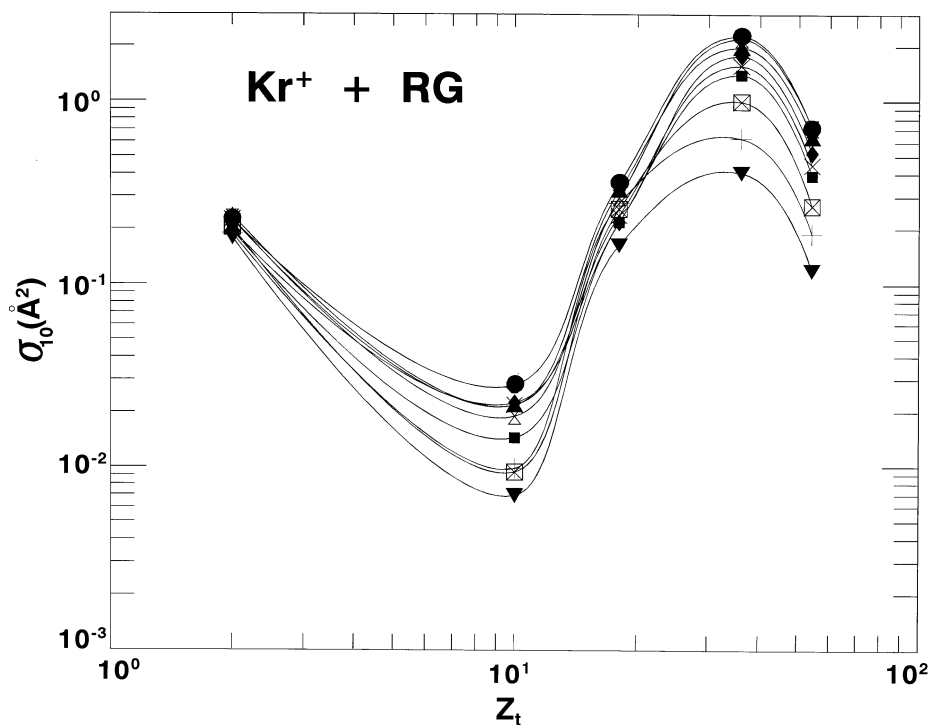


Fig. 4. Total cross sections for single electron capture of Kr^+ ions in rare gases as a function of the target atomic number. Down-pointing triangles, 1.0 keV; plus signs, 1.5 keV; boxed multiplication sign, 2.0 keV; squares, 2.5 keV; multiplication sign, 3.0 keV; diamonds, 3.5 keV; triangles, 4.0 keV; hourglasses, 4.5 keV; circles, 5.0 keV.

References

- [1] D. R. Sieglaff, B. G. Lindsay, K. A. Smith, R. F. Stebbings, *Phys. Rev. A* 59 (1999) 3538; G. J. Smith, R. S. Gao, B. G. Lindsay, K. A. Smith, R. F. Stebbings, *Phys. Rev. A* 53 (1996) 1581.
- [2] J. P. Gu, G. Hirsch, R. J. Buenker, M. Kimura, C. M. Dutta, P. Nordlander, *Phys. Rev. A* 59 (1999) 405.
- [3] A. Kolakowska, M. S. Pindzola, D. R. Shultz, *Phys. Rev. A* 59 (1999) 3588.
- [4] M. Barat, J. Baudon, M. Abignoli, J. C. Houver, *J. Phys. B* 3 (1970) 230.
- [5] G. Gerber, A. Niehaus, B. Steffan, *J. Phys. B* 6 (1973) 1836.
- [6] V. Sidis, M. Barat, D. Dhucq, *J. Phys. B* 8 (1975) 474.
- [7] W. B. Maier II, *J. Chem. Phys.* 69 (1978) 3077.
- [8] R. Solanki, E. L. Latush, D. C. Gerstenberger, W. M. Fairbank Jr., G. J. Collins, *Appl. Phys. Lett.* 35 (1979) 317.
- [9] M. Tsuji, N. Kaneko, M. Furusawa, T. Muraoka, Y. Nishimura, *J. Chem. Phys.* 98 (1993) 8565.
- [10] M. Tsuji, N. Kaneko, Y. Nishimura, *J. Chem. Phys.* 99 (1993) 4539.
- [11] H. Martínez, J. M. Hernández, *J. Chem. Phys.* 215 (1997) 285.
- [12] H. Martínez, J. M. Hernández, P. G. Reyes, E. R. Marquina, C. Cisneros, *Nucl. Instrum. Methods Phys. Res. B* 124 (1997) 464.
- [13] H. Martínez, P. G. Reyes, *Phys. Rev. A* 59 (1999) 2504.
- [14] H. Martínez, *J. Phys. B: At. Mol. Opt. Phys.* 32 (1999) 189.
- [15] H. Martínez, *J. Phys. B: At. Mol. Opt. Phys.* 31 (1998) 1553.
- [16] F. T. Smith, R. P. Marchi, W. Aberth, D. C. Lorents, O. Heinz, *Phys. Rev.* 161 (1967) 31; F. T. Smith, R. P. Marchi, K. G. Dedrick, *Phys. Rev.* 150 (1966) 79.
- [17] I. S. Dimitriev, N. F. Vorobiev, V. P. Zaikov, Zh. M. Konovalova, V. S. Nikolaev, Ya. A. Teplova, Yu. A. Fainberg, *J. Phys. B: At. Mol. Opt. Phys.* 15 (1982) L351.
- [18] F. Bell, H. D. Betz, *J. Phys. B: At. Mol. Opt. Phys.* 10 (1977) 483.